6th International Symposium on Three-Dimensional Electromagnetics
Berkeley, California, USA, March 28-30, 2017

High resolution cross-hole electromagnetic imaging with contrast source inversion

Yongxing Li and Richard S. Smith
Laurentian University

SUMMARY

We propose to use the 2D contrast source inversion (CSI) method for cross-hole radio imaging (RIM) data. The contrast source is defined as the product of the electric field and the object profile, the latter of which contains information about the conductivity and the permittivity of a model. A quadratic cost function is built and minimized with the conjugate gradient iterative method by alternatively updating the contrast source and the object profile. To demonstrate the effectiveness of the CSI method, we applied the method to synthetic data generated from a 3D model calculated with a finite element modelling package (Comsol Multiphysics). The synthetic model has a perfect conductor and a moderate conductor embedded in a layered background. From the inverted conductivity model, we can correctly interpret the boundaries and the interfaces of the layers, as well as the locations and the orientations of the conductors; but the conductivity values cannot be correctly estimated. It takes only 6.5 minutes to invert the data of the synthetic model using 400 iterations, which is significantly less than the computation time for generating the 3D synthetic data, and realistic for practical use.

Keywords: Contrast source inversion, cross-hole, back scattering, electromagnetic, 2D inversion

INTRODUCTION

Cross-hole electromagnetic (EM) exploration methods have been used to delineate ore bodies, detect mining hazards and select sites for underground nuclear waste disposal (Mutton, 2000; Korpisalo, 2016). In mining exploration, radio-frequency EM waves (typically 0.1 to 10 MHz) are often used and the method is known as the radio-imaging method (RIM) (Li and Smith, 2015).

Currently, the straight-ray imaging method is the primary interpretation method for RIM data. Li and Smith (2015) modelled the RIM data with a finite element modelling package, Comsol Multiphysics, and assessed the straight-ray imaging method with synthetic data (Li and Smith, 2016, submitted paper), which showed that the straight-ray method is not always appropriate for RIM data interpretation.

Compared with RADAR methods, the radio-frequency EM waves have lower frequencies and longer wavelengths. It is more appropriate to describe the radio-frequency EM problem as a back scattering problem, rather than a ray propagation problem. The EM back scattering inversion was developed in the 1990s' for tumours diagnosis (Joachimowicz et al., 1991), which is now developed into two categories of methods: one based on a Gauss-Newton frame work (Mojabi et al., 2011) and one based on contrast source inversion (CSI) (van den Berg and Kleinman, 1997; van den Berg et al., 1999; Abubakar et al., 2002).

In this paper, we will introduce the CSI algorithm for the RIM data. In the section SYNTHETIC STUDY, we will assess the effectiveness of this method using synthetic data generated for a 3D model with Comsol Multiphysics.

CONTRAST SOURCE INVERSION

The borehole plane is meshed with rectangular cells (Figure 1), each of which has uniform conductivity σ, permittivity ε, and electric field. The total electric field $\boldsymbol{E}^{total}(\boldsymbol{x})$ is decomposed to an incident field $\boldsymbol{E}^{inc}(\boldsymbol{x})$ from the source and a scattered field $\boldsymbol{E}^{sct}(\boldsymbol{x})$ from the anomalies in the model (Figure 1a),

$$\boldsymbol{E}^{total}(\boldsymbol{x}) = \boldsymbol{E}^{inc}(\boldsymbol{x}) + \boldsymbol{E}^{sct}(\boldsymbol{x}). \quad (1)$$

$\boldsymbol{x}$ denotes the position of the electric fields. The relation between the scattered field from all the cells in the model and the total fields of the cells in the model satisfies the integral equation (Joachimowicz et al., 1991; van den Berg et al., 1999),

$$\boldsymbol{E}^{sct}(\boldsymbol{x}) =$$

$$(k_0^2 + \boldsymbol{\nabla}^R\boldsymbol{\nabla}^R)\int_D g(\boldsymbol{x}-\boldsymbol{x}')\chi(\boldsymbol{x}')\boldsymbol{E}^{total}(\boldsymbol{x}')dv(\boldsymbol{x}'), \quad (2)$$

where, k is the wavenumber: $k^2 = \mu\omega^2\varepsilon - i\mu\omega\sigma$, in which μ is the magnetic permeability (in this study, we assume $\mu \equiv 1.2566370614 \times 10^{-6}$ H/m); k_0 is the wavenumber of the background; $\omega = 2\pi f$, is the angular frequency, where, f is the frequency;

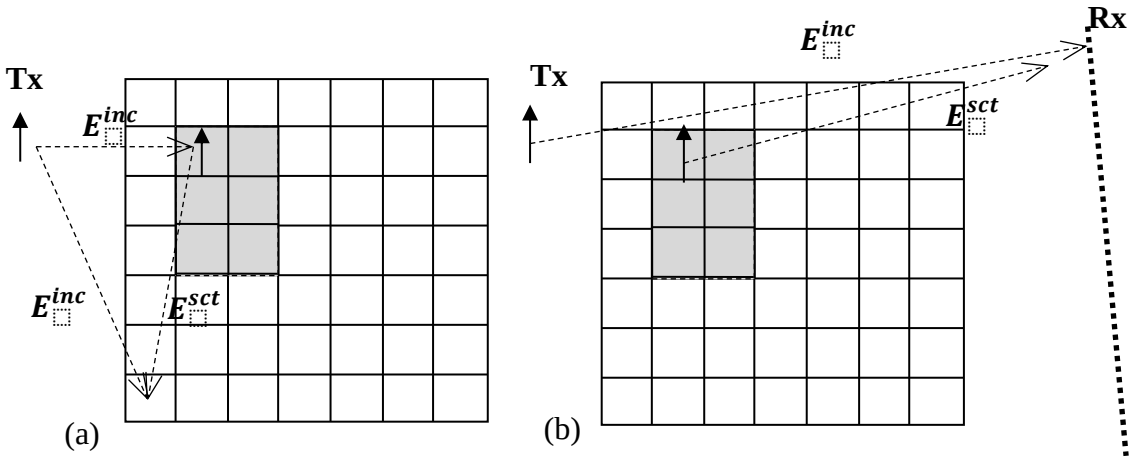

Figure 1. Discretization of a borehole plane for inversion. (a) Scattered field from a cell to another cell; (b) scattered field from a cell to a receiver location.

$\chi(\boldsymbol{x}) = (k^2(\boldsymbol{x}) - k_0^2)/k_0^2$ is the object profile; g is the Green's function: in the 2D case,

$$g(\mathbf{r}) = -\frac{i}{4}H_0^{(2)}(k_0|\mathbf{r}|), \tag{3}$$

where, $H_0^{(2)}$ is the zeroth order Hankel function of the second kind.

By substituting eq. (1) into eq. (2), a set of equations about the total fields for the cells in the model can be built. By solving the equations, the electric field for each cell can be obtained. After that, we can use eq. (2) again to calculate the scattered field at a receiver location (Figure 1b), and hence the total field.

However, the equations are highly nonlinear. To speed up the inversion, we introduce the CSI algorithm (van den Berg and Kleinman, 1997; van den Berg et al., 1999; Abubakar et al., 2002). The contrast source is defined as,

$$w_i(\boldsymbol{x}) = \chi(\boldsymbol{x})u_i^{total}(\boldsymbol{x}), \tag{4}$$

where, u_i^{total} is a simplified notation for the total electric field with the incident field coming from the i^{th} transmitter. The equation to calculate the scattered field at the receiver location from the model (eq. (2)) becomes,

$$f_i = G_S w_i, \tag{5}$$

where, G_S is a matrix, each element of which is a dyadic Green's function with the source at a cell and the receiver in a borehole. The equation combining eq. (1) and (2) becomes,

$$\chi u_i^{inc} = w_i - G_D \chi w_i, \tag{6}$$

where, u_i^{inc} is the incident field; G_D is a matrix, each element of which is a dyadic Green's function with the source location and the evaluation location in the cells of the model.

We define a cost function by combining eq. (5) and (6).

$$F_n(w,\chi) = \eta^S \sum_i \left\| f_i - G_S w_i \right\|_S^2 + \eta^D \sum_i \left\| \chi u_i^{inc} - w_i + \chi G_D w_i \right\|_D^2, \tag{7}$$

where,

$$\eta^S = \left(\sum_i \left\| f_i \right\|^2 \right)^{-1}, \tag{8}$$

$$\eta^D = \left(\sum_i \left\| \chi_{n-1} u_i^{inc} \right\|^2 \right)^{-1}, \tag{9}$$

in which, $\| \quad \|^2$ denotes the L-2 norm. Equation (7) is a quadratic function. We follow van den Berg et al. (1999) and use the conjugate gradient method to update the contrast source w and the object profile χ alternatively.

SYNTHETIC STUDY

To demonstrate the effectiveness of the CSI method for RIM data, we build a 3D model in Comsol Mutiphysics (Li and Smith, 2015) with two conductors embedded in a layered background. The geometry of the borehole plane (y = 0) is shown in Figure 2a: the background is a three-layered model; the upper layer and the lower layer have a conductivity of 0.001 S/m; the center layer has a conductivity of 0.0001 S/m; the two conductors are embedded in the center layer; conductor 1 is a perfect conductor; conductor 2 has a conductivity of 0.01 S/m. Both conductors are rectangular prisms with a strike length of 60 m (from y = -30 m to y = 30 m). Conductor 1 has an intersection of 80 m × 30 m in the borehole plane; conductor 2 has an intersection of 75 m × 25 m.

Two sub-vertical boreholes are on either side of the borehole plane. The "domain of interest" for Comsol is defined as a prism of 215 m × 340 m × 60 m, which includes the two boreholes and five sub-domains. To calculated the synthetic data, we mesh each sub-domain with element sizes that are between 1/5 to 1/7 of the wavelength, except the sub-domain of conductor 1 (perfect conductive boundary condition). The expected errors in the synthetic data are less than 5% (Li and Smith, 2015). We simulate a RIM survery with receivers spaced at 5 m intervals in one borehole and transmitters every 20 m in the other hole. The transmitting frequency is 2.5 MHz, which is one of the operating frequencies of

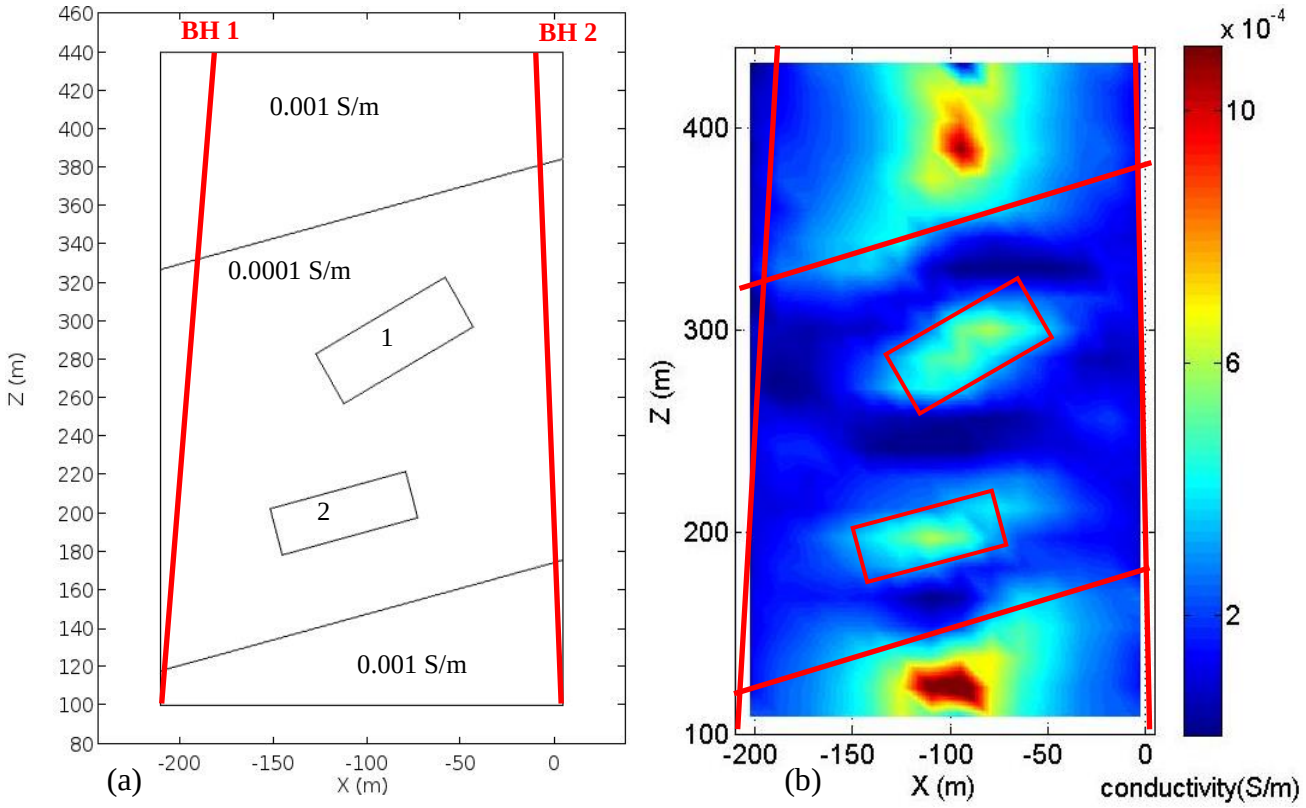

Figure 2. (a) The borehole plane section view of the synthetic 3D model with conductor 1 (perfect conductor) and conductor 2 (with a conductivity of 0.01 S/m) in a layered background. The strike length of the two conductors is 60 m and both are symmetric across the borehole plane ($y = 0$). (b) Inverted conductivity model.

the FARA system (Li and Smith, 2015). The dipole moment of the source is 4000 Am.

In the inversion, we mesh the 215 m × 340 m borehole plane with 322 cells, each of which is a rectangle of size 15.4 m × 14.8 m. During the inversion, the cost function converges stably and arrives at a value of 0.0015 after 400 iterations. No significant improvement in the results can be observed with further iterations.

The inverted conductivity model is shown on Figure 2b. The central parts of the top layer and the bottom layer have the highest conductivity value. Even though the distribution of conductivity within these layers is not constant, we can still interpret the boundaries and the angles of the tilted interfaces from Figure 2b. In the inversion section, conductor 1 is clearly shown in the correct position, with the shape and orientation roughly correct. There is a conductive area at the center position of conductor 2 and the shape and orientation are also roughly correct, but the right boundary of conductor 2 is poorly resolved. The slightly poorer result is likely because the lower conductivity of conductor 1 results in weaker scattered fields. There are low conductivity areas between adjacent conductors, which can be used to identify the zones as separate conductors within the inverted conductivity model.

The highest inverted conductivity value of the two conductors in the center layer is about 0.0006 S/m, which is much lower than the true values (infinite and 0.01S/m), and even lower than the inverted conductivity values of the upper layer and the lower layer (over 0.001 S/m). We speculate that the high inverted conductivity of the upper and lower layer is caused by the large volume, which highly attenuate the EM fields. Although the correct conductivity value of the conductors cannot be interpreted from the inverted conductivity model, we conclude that the inverted conductivity model obtained with the CSI method is helpful to interpret the location and the shape of the conductive zones between two boreholes with high resolution.

DISCUSSIONS AND CONCLUSIONS

We presented the CSI algorithm for RIM data, and developed an inversion program in C#. The program is implemented on a dual-core computer with a clock speed of 2.6 GHz. For the above example, it takes 6.5 minutes for 400 iterations. These run times should be compared to the 3D forward modelling with Comsol, which takes around 90 minutes to calculate the data from only one transmitter location (there are 36 transmitter locations in total) using an 8-core computer with a clock speed of 2.6 GHz. We argue that the CSI method is quite fast and it is a practical method to use to invert RIM data.

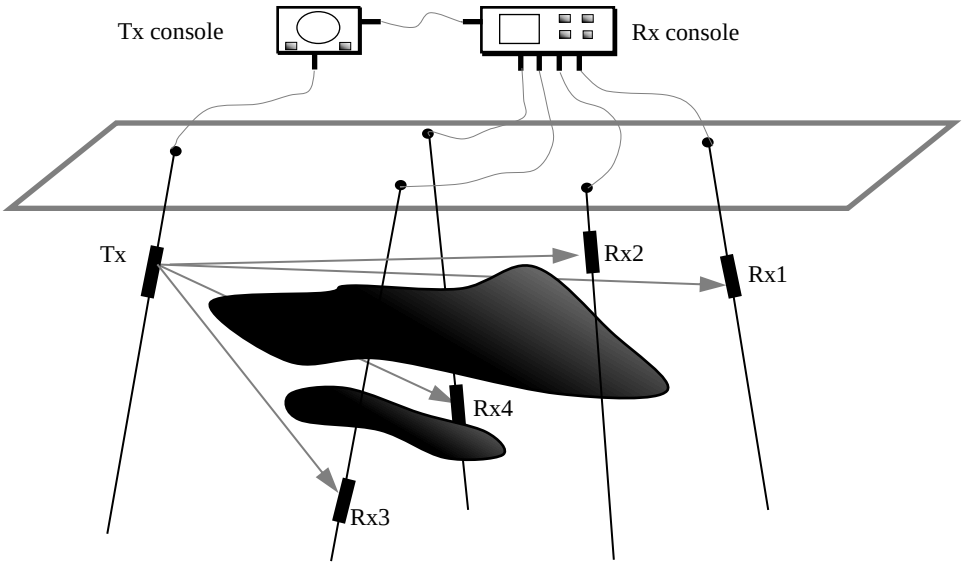

Figure 3. Schematic diagram of a 3D cross-hole EM exploration system with a transmitter (Tx) in one borehole and multiple receivers (Rx) in multiple boreholes.

The inversion results on this synthetic model are very encouraging, as this model is very similar to situations that might be encountered in mineral exploration. The features that can be identified using transmitters and receivers on either side of the zone of interest are much more detailed that are normally seen when the transmitters and the receivers are on the surface.

Although the CSI presented in this paper is limited to 2D, the CSI method can be extended to 3D using different Green's functions (Joachimowicz et al., 1991; Abubakar, et al., 2002). However, 3D exploration requires information from more than two boreholes. To our knowledge, the cross-hole EM instruments available to the mining industry only have one transmitter and one receiver (Li and Smith, 2015; Korpisalo, 2016). We encourage the development of a more versatile instrument with multiple receivers (Figure 3), which can be used to receive signals in multiple boreholes. With the data collected from such a tool, and the 3D inversion methods (yet to be developed and tested), we will benefit from high resolution 3D EM imaging techniques in the near future.

ACKNOWLEDGMENTS

The authors express acknowledgments to the Natural Sciences and Engineering Research Council of Canada (NSERC), Vale, KGHM International, Sudbury Integrated Nickel Operations -- A Glencore Company, Wallbridge Mining and the Centre for Excellence in Mining Innovation for funding this research.

REFERENCES

Abubakar, A., van den Berg, P.M. and Mallorqui, J.J., 2002, Imaging of biomedical data using a multiplicative regularized contrast source inversion method, *IEEE Transactions on Microwave Theory and Techniques*, **50**(7), 1761-1771.

Joachimowicz, N., Pichot, C. and Hugonin, J. P., 1991, Inverse scattering: an iterative numerical method for electromagnetic imaging, *IEEE Transactions on Antennas and Propagation*, **39**(12), 1742-1753.

Korpisalo, A.L., 2016, *Electromagnetic Geotomographic Research on Attenuating Material Using the Middle Radio Frequency Band*, PhD dissertation, University of Helsinki.

Li, Y. and Smith, R. S., 2015, Forward modeling of radio imaging (RIM) data with the Comsol RF module, *Computers & Geosciences*, **85**, 60-67.

Mojabi, P., LoVetri, J. and Shafai, L., 2011, A multiplicative regularized Gauss–Newton inversion for shape and location reconstruction, *IEEE Transactions on Antennas and Propagation*, **59**(12), 4790-4802.

Mutton, A. J., 2000, The application of geophysics during evaluation of the Century zinc deposit, *Geophysics*, **65**(6), 1946-1960.

van den Berg P.M. and Kleinman, R.E., 1997, A contrast source inversion method, *Inverse Problems*, **13**(6), 1607-1620.

van den Berg, P.M., Van Broekhoven, A.L. and Abubakar, A., 1999, Extended contrast source inversion, *Inverse Problems*, **15**(5), 1325 - 1344.